

A high-resolution, spatially explicit estimate of fossil-fuel CO₂ emissions from the Tokyo Metropolis, Japan

Richao Cong (✉ richao.cong@nies.go.jp)

National Institute for Environmental Studies <https://orcid.org/0000-0002-6315-6147>

Makoto Saito

National Institute for Environmental Studies

Tomohiro Oda

NASA Goddard Space Flight Center; Universities Space Research Association

Tetsuo Fukui

Institute of Behavioral Sciences

Ryuichi Hirata

National Institute for Environmental Studies

Akihiko Ito

National Institute for Environmental Studies

Methodology

Keywords: Carbon dioxide, CO₂ emission inventory, Fossil fuel, GIS, High-resolution map, Tokyo emissions

Posted Date: March 23rd, 2020

DOI: <https://doi.org/10.21203/rs.3.rs-17565/v1>

License: © ⓘ This work is licensed under a Creative Commons Attribution 4.0 International License. [Read Full License](#)

Abstract

Background: The quantification of urban greenhouse gas (GHG) emissions is an important task in combating climate change. Emission inventories that include spatially explicit emission estimates facilitate the accurate tracking of emission changes, identification of emission sources, and formulation of policies for climate-change mitigation. Many currently available gridded emission estimates are based on the disaggregation of country- or state-wide emission estimates, which may be useful in describing city-wide emissions but are of limited value in tracking changes at subnational levels. Urban GHG emissions should therefore be quantified with a true bottom-up approach.

Results: Multi-resolution, spatially explicit estimates of fossil-fuel carbon dioxide (FFCO₂) emissions from the Tokyo Metropolis, Japan, were derived. Spatially explicit emission data were collected for point (e.g., power plants and waste incinerators), line (mostly traffic), and area (e.g., residential and commercial areas) sources. Emissions were mapped on the basis of emission rates calculated for source locations. Activity, emissions, and spatial data were integrated, and the results were visualized using a geographic information system approach.

Conclusions: The annual total FFCO₂ emissions from the Tokyo Metropolis in 2014 were 44,855 Gg CO₂, with the road-transportation sector (16,323 Gg CO₂) accounting for 36.4% of the total. Spatial emission patterns were verified via a comparison with the East Asian Air Pollutant Emission Grid Database for Japan (EAGrid-Japan), which demonstrated the applicability of this methodology to other prefectures and therefore the entire country.

Background

Fossil-fuel combustion is a major contributor to increasing atmospheric carbon dioxide (CO₂) concentrations [1], with cities worldwide being responsible for more than 70% of the global total fossil-fuel CO₂ emissions (FFCO₂) [2]. As large sources of FFCO₂, cities have great potential for emission mitigation [3]. In response to the need for local climate action, many global cities have participated in climate action groups, such as the C40 Cities Climate Leadership Group [4] and the Global Covenant of Mayors for Climate & Energy [5], and started compiling emission inventories (EIs). The EIs are often compiled following the Global Protocol for Community-Scale Greenhouse Gas Emission Inventories (GPC) [6].

The Paris Agreement of the United Nations Framework Convention on Climate Change (UNFCCC) recognizes the importance of climate-change mitigation at subnational levels [7]. However, subnational emission estimates (e.g., state, province, city (UN-Habitat [2]), and private sector) are beyond the scope of the current Intergovernmental Panel on Climate Change (IPCC) guidelines. The inventory framework implemented under the Kyoto Protocol focuses on national compliance with global emission-reduction targets [8], rather than monitoring emission changes at subnational levels.

Subnational emission estimates can be obtained from spatially explicit emission data. Gurney et al. [9] loosely categorized emission modeling approaches as 'downscaled' or 'mechanistic'. In general, emission estimates using mechanistic approaches are more suitable for tracking emission changes in local areas. For example, emissions in the National geoinformation technologies, temporospatial approaches, and the Protocol for Reducing GHG Emission Uncertainties (GESAPU) are calculated at the locations of sources (e.g., points, lines, and areas) [10], taking into account the emission processes. Thus, GESAPU estimates can be used to keep track of local emission changes over the domain of a single country. In the US, Gurney et al. have developed city-scale emission data for several cities, including Indianapolis [11], Los Angeles [12], Salt Lake City [13], and Baltimore [14] under the Hestia Project. In Japan, Mori [15] developed a multi-resolution fossil-fuel CO₂ emission model for Osaka.

This paper presents the first spatially explicit FFCO₂ emission data for the Tokyo Metropolis (population 13.6 M in 2016; area 2,189 km²) for the year 2014. We distinguish our work from the East Asian Air Pollutant Emission Grid Database for Japan (EAGrid-Japan) by the use of a multi-resolution approach and updated information. We describe varieties of statistical and geospatial data used in estimating and mapping emissions, and compare our emission estimates with existing estimates at aggregated city and grid cell levels. We also discuss current limitations and future improvements.

Methods

Emission definition and modeling framework

The focus here is on quantifying FFCO₂ emissions from the Tokyo Metropolis using the modeling framework described in Fig. 1. Following previous studies [10, 11, 15], a multi-resolution emission modeling approach was employed, where CO₂ emissions ('emissions' hereinafter) were calculated on an individual source basis in a bottom-up manner, rather than using aggregated emission-sector levels. Emissions were spatially allocated using verified geographic latitude and longitude coordinates (mainly for point sources) and spatial geolocation data (for line and area sources), with examples of point-source locations and geospatial data shown in Fig. 2.

The total emissions for the year 2014 were calculated using the best available locally collected data following the 2006 IPCC guidelines [16]. Emission sources therefore included electricity generation (IPCC code 1A1ai), civil aviation (1A3a), waterborne navigation (1A3d), waste incineration (4C1), road transportation (1A3bi, 1A3bii, and 1A3biii), industrial and commercial sources (1A1aiii, 1A2, 1A4a, and 1A4ciii), residential sources (1A4b), and agricultural machine use (1A4cii). These emissions were calculated using the Tier 3 approach [16]. The emission-sector definitions, spatial information and data, activity data, and emission factors are summarized in Table 1.

Table 1

Spatial data used for identifying CO₂ emission sources, and other data used for counting emissions for each sector in Tokyo. Note that several sectors are not consistent with the IPCC definitions. For example, (1) only the LTO cycle emissions were used here for civil aviation, whereas the IPCC sector includes emissions from LTO cycle and cruise; (2) only passenger and cargo ships with round trips to the ports were considered here for the waterborne navigation sector, whereas the IPCC sector covers all water-borne transport, from recreational craft to large ocean-going cargo ships; and (3) two IPCC sectors (manufacturing and commercial sectors) were combined to form the industrial and commercial sector.

Emission sector (IPCC sector code)	Source type	Spatial information	Activity and spatial data	Emission factor
Electricity generation (1A1ai)	Point	Center points of chimneys of power plants (latitude, longitude)	Capacity and generation types of fossil-fuel power generation [17–20], and running ratio [21]	Emission factors of fossil-fuel power generation [22, 23]
Civil aviation (1A3a)	Point	Representative points of runways at airports (latitude, longitude)	Annual flight numbers [24], aircraft types, engine types, number of engines [25–33], and flight timetables [34, 35]	Energy consumption intensity of aircraft by engine type [16, 36, 37]
Waterborne navigation (1A3d)	Point	Representative points of buildings at ports (latitude, longitude)	Load factors, fuel consumption time [38, 39], and trips by vessels [40, 41]	Emission factors of vessels by vessel type [23, 38, 39]
Waste incineration (4C1)	Point	Center points of chimneys at waste incineration plants (latitude, longitude)	CA consumption rate [42], MSW combustion amount [43], industrial waste combustion amount [44], and disposal capacity [45]	Emission factors of fossil-carbon content by type [23]
Road transportation (1A3bi, 1A3bii, and 1A3biii)	Line	Length (m), width, and road types of the central road lanes	Traffic conditions [46], road lengths from DRM [47], and administrative map of Tokyo [48]	Emission factors of vehicles by vehicle speed and type [49]
Industrial and commercial (1A1aiii, 1A2, 1A4a, and 1A4cii)	Area	Site area (m ²), height, and number of floors in industrial and commercial buildings	Worker numbers [52], energy-balance table [53], land use map of Tokyo [55], DSM [56], and building polygons and DEM [57]	Emission factors of workers by industry category [52, 53]
Residential (1A4b)	Area	Site area (m ²), height, and number of floors in residential buildings	Land use map of Tokyo [55], DSM [56], building polygons and DEM [57], and household occupancy [58]	Emission factors of households by building type and occupancy [59]
Agricultural machinery use (1A4cii)	Area	Area of cultivated lands by crop type (area)	Administrative map of Tokyo [48], area of cultivated land by crop type [60], and high-resolution land use map [63]	Emission factors of farmlands by crop type [61, 62]

Point-source emissions

Point-source emissions include those from electricity generation, civil aviation, waterborne navigation, and waste incineration (Table 1). For electricity generation, only fossil-fueled power plants in Tokyo ($n = 19$) were considered (see Additional File 1; Table S1 for details). The 2014 total emissions from all power plants were calculated by formula:

$$E_{eg} = 24 \cdot \sum_{i=1}^n \sum_{j=1}^{12} C_i \cdot D_j \cdot R_{g,j} \cdot EF_{g,j},$$

1

where E_{eg} represents the total annual emissions from electricity generation (Gg CO₂); the coefficient 24 indicates the number of hours per day; C_i is the electricity generation capacity (kW) of power plant i in Tokyo with one type of generator (steam, gas cogeneration, or internal combustion); D_j is the number of days in month j ; $R_{g,j}$ is the mean operating ratio of fossil-fueled power plants with generator type g in month j for 2014; and $EF_{g,j}$ is the emission factor for fossil-fueled electricity generation by generator type g in month j (Gg CO₂ kWh⁻¹). The C_i values were obtained from the Electrical Japan Database (data were collected in April 2017) [17] and operator companies [18–20]. The $R_{g,j}$ values are reported by power plant operators and published by the government of Japan each year [21]. The emission factors of power plants in 2014 ($EF_{g,j}$) were derived from electricity generation amounts by power plants, the monthly fuel consumption (e.g., coal, crude oil, heavy oil, light oil, liquefied natural gas, liquefied petroleum gas, and other gas) [22], and official guidelines for GHG emissions counting [23]. Where there was a lack of individual data for a plant, R_j and EF_j values for plants with the same type of generator were used. The stack centroid was used as the representative emission location for multiple smoke stacks in a single power plant facility. An example of point-source emissions in SG Ward (see Table S2) is shown in Fig. 2A.

Civil aviation emissions included those from passenger and cargo aircraft during landing and take-off (LTO) at an international airport, four helipads, and six domestic airports (Table S1). The 2014 total emissions from LTO movements were calculated as follows:

$$E_{ca} = 2 \cdot \sum_{i=1}^n \sum_a F_{a,i} \cdot N_a \cdot EC_e \cdot EF_f,$$

2

where E_{ca} represents the total annual emissions from civil aviation (Gg CO₂); $F_{a,i}$ is the total number of arrivals for type a aircraft with one type of engine at airport i in 2014 (the coefficient 2 indicates landings = departures in LTO cycles); N_a is the number of engines on type a aircraft; EC_g is the jet fuel ('energy') consumption per engine during an LTO cycle by engine type e (Gg per engine per LTO); and EF_f is the emission factor of jet fuel (3.154 Gg CO₂ Gg⁻¹) [23]. The $F_{a,i}$ and N_a values were summarized from 2014 flight records [24–32] and websites [33]. The monthly proportion of aircraft types at Haneda airport was used as the annual proportion for 2014 due to the lack of annual flight timetables for each aircraft type. The monthly proportions of arrivals for each aircraft type were obtained from flight timetables for April 2017 [34, 35]. The EC_g values were extracted from the Aircraft Engine Emissions Databank of the International Civil Aviation Organization (ICAO) [36] and guidance on helicopter emissions [16, 37]. As aircraft are mobile sources, the calculated emissions were mapped using representative points on airport runways (diameter ~ 1 km) as point sources.

Emissions from the waterborne navigation sector included emissions from fuel consumed by vessels during round trips to ports in Tokyo ($N= 15$; Table S1). The 2014 total emissions from vessels were calculated as follows:

$$E_{wn} = \sum_{i=1}^n \sum_{t,m} I_{t,m} \cdot R_{t,m} \cdot T_{t,m} \cdot N_{t,i} \cdot EF_t.$$

3

where E_{wn} represents the total annual emissions by vessels (Gg CO₂); $I_{t,m}$ is the emission intensity of fuels (tonne per vessel) for type t vessels (including merchant vessels, car ferries, evacuation vessels, fishing vessels, and other vessels) at mode M (travelling, mooring, cargo loading, and unloading); $R_{t,m}$ is the load factor of type- t vessels in mode M ; $T_{t,m}$ is the fuel consumption time of type- t vessels in mode M (h); $N_{t,i}$ is the annual number of type- t vessels travelling to port i ; and EF_t is the emission factor (Gg CO₂ tonne⁻¹) for type- t vessels consuming heavy oil or light oil. The $I_{t,m}$, $R_{t,m}$ and $T_{t,m}$ values and the average travel speed for these vessels were obtained from technical reports [38, 39]. As shown by the parameters listed in Table S3, the mean travel distance was assumed to be 1 km in travelling mode to derive the travel time. The emissions from travelling mode were considered for fishing vessels but all mode were considered for the other types of vessels. The $N_{t,i}$ values were obtained from statistical data on vessels in ports [40, 41]. The EF_t data were extracted from the official guideline [23]. As waterborne vessels are mobile sources, representative points on port buildings were used as their point-source locations.

Emissions from incineration plants do not contribute to FFCO₂ emissions. However, this study included their emissions because the emission intensity is significant. Emissions from incineration plants for municipal solid waste (MSW, $N= 46$) and industrial waste ($N= 15$) (Table S1) included those from the combustion of wastes containing carbon (e.g., papers, plastics, textiles, rubbers, and oil) and the combustion agent (CA, "city gas" comprising liquid petroleum gas and natural gas). Emissions from MSW waste combustion were calculated as follows:

$$E_{mw} = \sum_{i=1}^n (\sum_c T_i \cdot R_{c,i} \cdot FC \cdot EF_c + T_i \cdot CR \cdot EF),$$

4

), where E_{mw} represents the 2014 total emissions from MSW incineration (Gg CO₂); T_i is the total amount of combustible content in waste (tonne) incinerated annually at plant i ; $R_{c,i}$ is the proportion of type- c content of waste (i.e., waste paper, plastic, rubber, and textiles in MSW) at plant i ; FC is the fossil carbon content in waste; EF_c is the emission factor for combustible content type c in waste (paper 1.69×10^{-5} ; plastic 2.55×10^{-3} ; textiles 2.29×10^{-3} ; rubber 1.72×10^{-3} Gg CO₂ tonne⁻¹) [23]; CR is the mean consumption of CA ($1.29 \text{ m}^3 \text{ tonne}^{-1}$) [42]; and EF is the emission factor for CA (2.21×10^{-6} Gg CO₂ m⁻³) [23]. The T_i and $R_{c,i}$ values for all 46 MSW incineration plants in Tokyo were obtained from the investigation report on MSW for Tokyo, 2014 [43]. Here we assumed that paper and textiles in wastes were in equal amounts and the fossil carbon content (FC) of these wastes were 50%. The CR values derived from available data for 19 MSW incineration plants in Tokyo [42] were used for all MSW incineration plants.

Emissions from industrial waste combustion were calculated as follows:

$$E_{iw} = \sum_c T_c \cdot FC \cdot EF_c,$$

5

), where E_{iw} represents the 2014 total emissions from industrial waste incineration (Gg CO₂); T_c is the total annual amount of combustible content in waste (tonnes) at all plants in Tokyo for type c (i.e., waste paper, plastic, textiles, and oil in industrial waste); and EF_c is the emission factor for fossil carbon in waste type c (oil 2.92×10^{-3} Gg CO₂ tonne⁻¹) [23]. T_c values were extracted from the investigation report on industrial waste incineration [44]. The FC value for industrial waste was assumed to be 1 with no CA used due to the high-purity carbon content. The emissions from 15 industrial-waste incineration plants were derived by allocating the E_{iw} with plant disposal capacities [45]. The central points of the chimneys at waste incineration plants were mapped as emission points.

Line-source emissions

Line-source emissions included those of the road-transport sector, based on traffic census data compiled by the Ministry of Land, Infrastructure, Transport and Tourism for each prefecture every five years, with the latest being in 2015 [46]. The census data include road information (name, width, length, number of lanes, and classification for each road segment), hourly and daily traffic volumes, and 12-h mean daytime vehicle speeds for small vehicles (light passenger cars, regular passenger cars, light trucks, and small freight cars) and large vehicles (bus, regular truck, and special-use vehicles). The road segment data indicate the network links, as shown in the example of a digital road map (DRM; [47]) in Fig. 2B. The census targets five road classifications: high-speed national highways, urban highways, general national highways, major regional roads (prefectural roads and designated city roads), and general regional roads. Emissions on minor roads that were not covered by the census were not considered.

Road transportation emissions were calculated for single road segments ($n= 45,564$) as follows:

$$E_{rt} = \sum_{i=1}^n \sum_v Q_{v,i} \cdot L_i \cdot EF_{v,s},$$

6

where E_{rt} represents the 2014 total emissions from road transportation (Gg CO₂); $Q_{v,i}$ is the annual traffic volume (derived from daily data) for type v vehicles at a vehicle speed (from 5 to 90 km/h) on road segment i ; L_i is the length of road segment i (km); $EF_{v,s}$ is the emission factor for type- V vehicles by vehicle speed s (Gg CO₂ km⁻¹ per vehicle). The census identification numbers for road segments were used with Google Maps software to select point coordinates for each observed road segment, with the selected points being mapped to identify the same roads on the DRM. The information from the traffic census, such as road classification, daily traffic volume, and mean speed, were combined for the DRM road segments. The average traffic conditions for each road classification in each municipality unit [48] were substituted for the road segments not covered by the census. The L_i values were calculated from the DRM using a geographic information system (GIS) tool. The $EF_{v,s}$ values were obtained from Dohi et al. [49] (Table 2). Emissions were mapped on the center line of each road segment.

Table 2

CO₂ emission factors for vehicles by vehicle type and speed (2010), extracted from experimental results [49].

Speed (km h ⁻¹)	CO ₂ emission factors for small vehicles (10 ⁻⁹ Gg CO ₂ km ⁻¹ per vehicle)	CO ₂ emission factors for large vehicles (10 ⁻⁹ Gg CO ₂ km ⁻¹ per vehicle)
5	437.1	1,646
10	328.8	1,372
15	237.1	1,099
20	209.8	1,014
25	187.5	928.7
30	171.3	855.7
35	158.9	793.7
40	149.5	741.9
45	142.2	700.1
50	136.9	667.9
55	133.2	645.4
60	131.1	632.3
65	130.3	628.6
70	130.9	634.3
75	132.8	649.3
80	135.9	673.6
85	140.2	707.2
90	145.6	750.1

Area-source emissions

Area-source emissions included those from the industrial, commercial, residential, and agricultural sectors. The main source of industrial, commercial, and residential emissions is fuel consumption in buildings, for which the Hestia project [14] estimated non-electrical energy using the eQUEST simulation tool [50] by incorporating the building classification and age, with the building emissions based on the building total floor areas (TFAs) [51].

Since spatial data (building polygons) are not available for buildings of all ages in Japan, census data were used to allocate the emissions using building polygons (Fig. 2C) based on the TFAs.

Emissions from the industrial and commercial sector included those from fossil-fuel consumption by workers. Emissions from all areas in Tokyo, based on the economic census ($n_{ca} = 5,318$), were calculated as follows:

$$E_{ic} = \sum_{i=1}^n \sum_q W_{q,i} \cdot \frac{TE_q}{TW_q},$$

7

where E_{ic} represents the 2014 total emissions from the industrial and commercial sector (Gg CO₂); $W_{q,i}$ is the number of workers for category q in census area i (Table 3); TE_q is the total annual emissions for category q (Gg CO₂); and TW_q is the total number of workers in category q . The $W_{q,i}$ values for all of the categories in census areas were obtained from the 2014 economic census [52]. The census area comprised politically based blocks with an average area of around 0.5 km². The TW_q values were obtained from economic census data [52], and the TE_q values were extracted from the Tokyo energy-balance table [53].

The annual CO₂ emission factors by workers (

$$\frac{TE_q}{TW_q},$$

Gg CO₂ per worker) were derived for each category (Table 3). The annual emissions from the fuels used in energy conversion (e.g., electricity generation and waste incineration) were not included in the energy-balance table [53] to avoid counting them twice. The total emissions for the industrial and commercial sector were allocated to every census area, similar to the approach used by Gately and Hutyra (2017) [54] with commercial emissions.

Table 3

Annual consumption of fossil fuels, worker numbers, and CO₂ emission factors for workers by category in Tokyo, derived from the 2014 economic census [52] and the energy-balance table for Tokyo (2014) [53].

Category	Fossil fuel consumption (Terajoules)	Annual emissions (Gg CO ₂ yr ⁻¹)	Total number of workers	CO ₂ emission factors 10 ⁻³ Gg CO ₂ yr ⁻¹ per worker)
Forestry and Fishery	4.6	16.9	4,151	4.1
Mining, Quarrying of Stone and Gravel	13.0	47.6	2,090	22.8
Construction Industry	234.0	857.9	465,553	1.8
Manufacturing, Auto Power Generation	730.2	2,678	713,594	3.8
Electricity, Gas, Heat Supply and Water	22.5	82.5	33,666	2.5
Information and Communications	67.2	246.3	833,221	0.3
Transport and Postal Activities	178.9	656.1	484,149	1.4
Wholesale and Retail Trade	329.2	1,207	1,996,425	0.6
Finance and Insurance	21.4	78.4	403,625	0.2
Real Estate and Goods Rental and Leasing	169.5	621.7	345,959	1.8
Scientific Research, Professional and Technical Services	70.6	258.7	474,795	0.5
Accommodation, Eating and Drinking Services	506.9	1,859	890,005	2.1
Living-Related and Personal Services and Amusement Services	369.4	1,354	353,091	3.8
Education, Learning Support	206.0	755.3	468,565	1.6
Medical, Health Care and Welfare	358.3	1,314	861,346	1.5
Compound Services	1.3	4.7	37,754	0.1
Miscellaneous Services	208.9	766.1	1,030,901	0.7
Government	79.0	289.6	258,416	1.1

Total emissions were allocated to individual buildings in each census area, with all of the building polygons being associated to a given building use (industrial and commercial, or residential), using land-use maps covering four areas (23 wards in Tokyo, the Tama city area, Tama rural area, and island areas) at spatial resolutions of 3 × 3 m to 43 × 43 m [55]. The data on individual building polygons (e.g., site area (m²), height (m), number of floors, and floor area (m²)) were obtained as follows. Each building site area was estimated from the building polygon maps, and the building height was estimated from the difference in heights between a raster-type digital surface model (DSM) [56] and a vector-type digital-elevation model (DEM) [57]. DSM v. 1.1 was based on digital photos from the Advanced Land Observing Satellite, with an accuracy within 5 m [56]. A 30 × 30 m DSM dataset was used with a 5 × 5 m DEM dataset (updated in 2016) based on airborne laser observations (2015), with an elevation accuracy within 0.7 m (standard deviation) [57]. The number of floors was estimated by dividing the building height by the average ceiling height (2.9 m for residential buildings, and 3.5 m for industrial and commercial buildings). The TFAs were estimated by multiplying the site area by the number of floors. The emission factors of the buildings (Gg CO₂ m⁻²) in each census area were calculated by dividing the total emissions by the TFAs, aggregated over the census areas. Finally, the emissions from each industrial and commercial building were estimated by multiplying the emission factors by the TFAs of the individual buildings. Industrial and commercial emissions were mapped at the level of individual buildings.

Emissions from the residential sector were calculated for all of the population census areas in Tokyo ($N = 5,578$) by formula:

$$E_{re} = \sum_{i=1}^n \sum_{f,h,b} A_{h,b,i} \cdot EF_{f,h,b}$$

8

where E_{re} represents the 2014 total emissions from the residential sector (Gg CO₂); $A_{h,b,i}$ is the number of households with occupancy h (with four categories: 1, 2, 3, or ≥ 4 occupants) in type b buildings (collective or detached) in the census area i , and $EF_{f,h,b}$ is the total annual emission intensity (Gg CO₂ yr⁻¹ per household) of fuel type f , in household with occupancy h , and for building type b . The $A_{h,b,i}$ values were obtained from the 2015 population census data [58], and the $EF_{f,h,b}$ were from an investigation report on energy consumption in households as provided in Table 4 [59]. Finally, the total emissions from each census area were allocated to each building in proportion to the TFAs and with consideration of whether the buildings were collective or detached, and mapped at the level of individual buildings.

Table 4

CO₂ emission factors for households by occupancy and building type, based on an investigation of residential energy consumption [59].

Household size (occupancy)	CO ₂ emission factors for detached buildings (10 ⁻³ Gg CO ₂ yr ⁻¹ per household)			CO ₂ emission factors for collective buildings (10 ⁻³ Gg CO ₂ yr ⁻¹ per household)		
	City gas	Liquefied petroleum gas	Kerosene	City gas	Liquefied petroleum gas	Kerosene
1	0.234	0.132	0.334	0.240	0.085	0.032
2	0.564	0.159	0.452	0.654	0.110	0.056
3	0.706	0.209	0.387	0.929	0.074	0.071
4 or more	0.809	0.257	0.379	1.120	0.106	0.069

Agricultural emissions in this study are defined as emissions from fossil fuel use in agricultural machinery. The emissions processes were considered as those arising during crop planting, and those associated emissions were calculated for 62 municipalities in Tokyo as follows:

$$E_{am} = \sum_{i=1}^n \sum_p A_{p,i} \cdot EF_p$$

9

where E_{am} represents the 2014 total emissions from agricultural machinery use (Gg CO₂); $A_{p,i}$ is the area for crop type i cultivated in municipality i (ha); and EF_p is the annual emission factor for farmland by crop type (Gg CO₂ ha⁻¹). The $A_{p,i}$ value for each Tokyo municipality was obtained from the agricultural

census in Tokyo [60], and the EF_p values were from a 2003 report [61] and an academic paper [62] (Table 5). Farmland was divided into two categories, rice paddy fields and other farmland, using a land-use map at a 10×10 m spatial resolution [63] based on remote-sensing data for the 2006–2011 period. Finally, the agricultural emissions mapped in each municipality [48] were sorted into a 10×10 m mesh for mapping based on the two types of farmland.

Table 5
CO₂ emission factors for farmland by crop type [61, 62].

Crop type	Emission factor (10 ⁻⁶ Gg CO ₂ ha ⁻¹ yr ⁻¹)
Rice cultivation	597.9
Wheat	727.7
Corn	338.0
Potato	719.3
Sweet potato	751.2
Red bean	414.6
Green soybean	499.7
Green tea	550.3
Japanese radish	922.8
Cabbage	1,488.2
Japanese mustard spinach	286.3
Italian ryegrass	458.5
Greenhouse tomato	124,200
Open-field tomato	1,744.2
Kosui Asian pear	1,330.5

Data integration

Emission calculations and spatial emissions mapping/modeling were integrated using ArcGIS v. 10.4. The world geodetic system (1984) was used for mapping all of the emission sources, and a symbol tool was used here for visualizing the emissions on maps. A 3D map of the emission sources in SG Ward is shown in Fig. 2D as an example, allowing visualization of the emissions from local facilities, road segments, and buildings.

All of the data used, their versions or editions, and sources are summarized in Table S4. More than two million building polygons were used to produce emission maps around 500 MB in size. The emission maps were not gridded products since a multi-resolution approach was adopted. The original maps were converted to a 1 km mesh size (Fig. 3) for convenience in data handling.

Results And Discussion

Total emissions from the Tokyo Metropolis

Tokyo is one of 47 prefectures in Japan and comprises 23 central city wards and multiple cities, towns, and villages (Table S2). The three highest point-source gridded emissions in 2014 occurred in SG, OT, and MN Wards at 6,183, 1,814, and 253 Gg CO₂ km⁻², respectively (Fig. 3A), due to two large power plants and a major airport being located within these areas. The highest line-source emissions occurred in KT, OT, and EG Wards at 155, 146, and 144 Gg CO₂ km⁻², respectively (Fig. 3B). The highest gridded emissions for area sources (Fig. 3C) occurred in CD, CO, and SJ Wards at 173, 168, and 164 Gg CO₂ km⁻², respectively. These high emissions are primarily due to the high floor numbers and large building areas for residential, industrial, and commercial use concentrated in these areas. A total emissions map is given in Fig. 3D, with the three highest emissions being 6,210 in SG Ward, 1,965 in OT Ward, and 295 Gg CO₂ km⁻² in MN Ward, respectively.

The estimated total 2014 FFCO₂ emissions from Tokyo were 44,855 Gg CO₂ (Table 6), which comprised individual sector contributions of 16,323 from road transportation; 13,085 from the industrial and commercial sector; 6,478 from electricity generation; 5,302 from the residential sector; 1,879 from civil aviation; 1,483 from waste incineration; 279 from waterborne navigation; and 26 Gg CO₂ from the agricultural machine use sector. Total annual emissions from the area, line, and point sources were 18,413, 16,323, and 10,119 Gg CO₂, respectively.

Table 6
Estimates of annual CO₂ emissions from Tokyo (2014) by sector and source type.

Sectors	IPCC sector code	Sectoral emissions (Gg CO ₂ yr ⁻¹)	Emission source type	Total emissions (Gg CO ₂ yr ⁻¹)
Electricity generation	1A1ai	6,478	Point source	10,109
Civil aviation	1A3a	1,879		
Waterborne navigation	1A3d	279		
Waste incineration	4C1	1,483		
Road transportation	1A3bi, 1A3bii, and 1A3biii	16,323	Line source	16,323
Industrial and commercial	1A1aiii, 1A2, 1A4a, and 1A4cii	13,085	Area source	18,413
Residential	1A4b	5,302		
Agricultural machine use	1A4cii	26		
Total	-	44,855		

The highest point-source emissions (Fig. 4) for 2014 were as follows. Power plants: Shinagawa (3,219), Oi (2,965), and Roppongi energy service (140 Gg CO₂) plants; Civil aviation: Haneda (1,814), Chofu (30), and Oshima (8 Gg CO₂) airports; Waterborne navigation: Tokyo (253), Mikurajima (5), and Okada (4 Gg CO₂) ports; and waste incineration plants: Tokyo Waterfront Recycle Power (188), Koto new plant (140), and Minato plant (89 Gg CO₂). The data for all 106 point sources are given in Table S1. The 19 power plants contributed 64.1% of the 2014 total point-source emissions (6,478), the 11 airports 18.6% (1,879), the 61 waste incineration plants 14.6% (1,483), and the 15 ports 2.8% (279 Gg CO₂).

The highest line-source emissions for 2014 (Fig. 5) were associated with 30 road segments on two urban highways: Central loop line highway in KS Ward (19.7) and the Coastline highway in KT Ward (18.8 Gg CO₂ km⁻¹). The 2014 emissions from high-speed national highways (total length 150 km) were 1,048 Gg CO₂ (6.4% of the total line-source emissions); urban highways (576 km) 4,867 Gg CO₂ (29.8%); general national highways (726 km) 3,520 Gg CO₂ (21.6%); major regional roads (1,625 km) 4,761 Gg CO₂ (29.2%); and general regional roads (1,614 km) 2,128 Gg CO₂ (13.0%).

The highest area-source emissions from the industrial and commercial sector for 2014 were recorded in the inner-city areas in CD (172.4), CO (167.0), and SJ (162.0 Gg CO₂ km⁻²) Wards (Fig. 6A), respectively. The industrial and commercial emissions counted from economic census areas were shown in Fig. 6B. Those from the residential sector were in KT (10.0), TS (9.9), and TT (9.5 Gg CO₂ km⁻²) Wards (Fig. 7A), respectively. The residential emissions counted from population census areas were shown in Fig. 7B. Those from the agricultural sector (Fig. 8A) were recorded in MS (0.45) and NK Cities (0.36), and EG Ward (0.33 Gg CO₂ km⁻²), respectively. The agricultural emissions counted for 62 municipalities (Fig. 8B) were finally allocated for high-spatial-resolution map (Fig. 8C).

Comparison with other emission estimates

The Tokyo government has reported annual GHG emissions every year since 1990, with emissions being calculated with a top-down approach based on energy consumption [64]. In the governmental EI, emissions for each sector in Tokyo are based on the final energy consumption, including electricity, city gas, liquefied petroleum gas, and kerosene, with emissions being apportioned according to economic indicators, such as family expenditure, commodity values, numbers of vehicles, buildings areas, and passenger and cargo transport in Tokyo.

Annual emissions between the present EI and the EI prepared by the Tokyo government [64] are compared for four major categories (Fig. 9A1-2). The governmental EI includes total emissions from the Tokyo Metropolis of 62,120 Gg CO₂ for 2014. The governmental EI includes the following emissions: 29,320 from the industrial and commercial sector; 19,650 from the residential sector; 11,570 from transportation; and 1,570 Gg CO₂ from waste incineration. Based on the annual emissions by sector and fuel type in the report [64], we derived the non-electric emissions for the residential sector from the governmental EI as 5,532, consistent with our result of 5,302 Gg CO₂. However, those for the industrial and commercial sector are different (governmental EI 6,080, the present EI 13,085 Gg CO₂). For waste incineration, the governmental EI considered only emissions from the fossil-carbon content of waste (1,570), whereas we included both these emissions (1,473) and the combustion agent (10 Gg CO₂).

The differences in emissions between the two EIs could be associated mainly with electricity production. This study estimated the emissions from electricity generation as point sources based on fossil-fuel consumption at power plants (direct emissions, Scope-1[6]), while the Tokyo government estimated them based on the final energy consumption (consumption-based emissions, Scope-2 [6]). For example, the government EI includes emissions from electricity consumption by railways and the electricity generated outside the Tokyo area [65]. These differences resulted in higher annual emissions from electricity consumption in the government EI (39,460) compared with the EI of the present study (6,478 Gg CO₂).

The EAGrid is a reliable EI for multiple pollutants that was developed for the East Asia region in 1995 [66] and revised in 2000 with a focus on local emission sources in Japan (EAGrid-Japan 2000) [67]. In the most recent version (2010), emissions were estimated by adjusting the 2000 emissions according to the increase in national fuel consumption from 2000 to 2010 (see Fukui et al. [68]), without any change in the distribution of emission sources. Here we relied on data for the Tokyo domain provided by the developer [68] of EAGrid-Japan 2010.

Total emissions in the EAGrid-Japan 2010 EI for Tokyo are 42,009, which is 6.3% lower than our estimate for 2014 (44,855 Gg CO₂). To compare the two sets of results by source type, the sectoral emissions of the present EI in three categories are summarized in Fig. 9B1 and those for EAGrid are shown in Fig. 9B2. The point-source emissions of EAGrid (5,631 Gg CO₂) include those from power plants, waste incineration plants, vessels, and aircraft; line sources from road transportation (14,672 Gg CO₂); and area sources (21,705 Gg CO₂) from residential and commercial combustion equipment, factory and building boilers, off-road transportation (construction, agricultural, and factory machine use), open burning, and facilities.

Spatial distributions of the emissions between the two EIs were compared at a 1 × 1 km resolution by scaling the total EAGrid emissions to our 2014 EI (Fig. 10). The difference in the point sources (Fig. 10A) shows that some gridded emissions of this study were lower than those in EAGrid. To map the gridded values of EAGrid, the counted total emissions from each airport and port were allocated by the area of the facility' boundary, with the number of point sources being higher than those in this study. Other differences are due to the EAGrid EI, which does not include recently constructed major sources, such as Shinagawa power plant and Haneda airport domestic terminal 2. As shown in Fig. 11A, the correlation of the gridded emissions of point sources between the two sets of results is very low ($R^2 = 0.31$).

Line-source differences (Fig. 10B) vary from - 100 to + 100 Gg CO₂ km⁻². The differences between the year of traffic census and road maps resulted in the difference in emissions. Road segment lengths were obtained from the 1995 DRM in the EAGrid EI [67], whereas we used the current 2015 versions. Area-source differences (Fig. 10C) are variable because the EAGrid EI includes residential, industrial, commercial, off-road, open burning, and other emissions as area sources, whereas this study only considers residential, industrial and commercial, and agricultural sectors as area sources. The area-source emissions in

the present EI were 3,292 Gg CO₂, lower than those of the EAGrid. As shown in Fig. 11B-C, the correlations of the gridded emissions for line and area sources between the two sets of results are high ($R^2 = 0.74$ for line sources and 0.71 for area sources).

Differences in total emissions vary between -1,500 and +4,500 Gg CO₂ km⁻² (Fig. 10D), with differences being smaller in the western mountain and forest areas and larger in the inner-city areas (eastern Tokyo). As shown in Fig. 11D, the correlation of the total gridded emissions between the two sets of results is moderate ($R^2 = 0.69$). The number of cells in the present EI is much greater than that in EAGrid in the 0–10 Gg CO₂ km⁻² emission range (Fig. 12), with the present EI therefore including more low-emission areas than the EAGrid, while greater 20–50 Gg CO₂ km⁻² emissions are included in the latter. The numbers of cells are consistent for the other emission ranges. Thus, we could conclude that even the number of cells in some emission ranges and the total annual emissions between the two sets of results seem to be close but the distributions of the source emissions are different.

Current limitations and future perspectives

Uncertainties associated with emission factors, activity data, and emission spatial modeling introduce uncertainties in the final emission estimates [e.g., 8, 69]. We refer to the uncertainties on the basis of activity data and emission factors (Table S5) using IPCC guidelines [16, 70]. The total uncertainty is estimated to be $\pm 3.57\%$, equivalent to $44,855 \pm 1,601$ Gg CO₂.

Uncertainties introduced from emissions calculations and mapping processes are likely to be large due to the assumptions and approximations used. For example, the operation ratio of power plants varies with individual plants; however, this study applied averaged operating ratios for the whole plants in the calculation process. This approach reduces the variability in emissions at each power plant, leading to poor representation of emissions with higher temporospatial resolution than we applied here. The road segments that are not fully covered by the census contribute over 4,205 km in our calculation. We substituted the average traffic conditions for the road segments to estimate the emissions. This approach could overestimate the traffic quantities and emissions for the segments.

In mapping processes, this study treated the mobile emissions of aircraft and vessels as point sources. This means that the whole emissions over their moving paths were aggregated to a point, leading to an overestimate of the point-source emissions. The building emissions were estimated using TFAs of buildings in each census area. In this estimate we used DSM data with a spatial resolution of 30 m, but this spatial resolution is insufficient to calculate the heights and TFAs for individual buildings. Additionally, our downscale approach did not distinguish occupied and vacant houses. All of these limitations should be improved in the next study. As in previous studies (e.g., Hestia [14]), better data availability for emissions calculations and mapping should greatly improve the accuracy of estimates.

We plan to update our emission estimates once updated activity data become available. The methods employed here are applicable to other parts of Japan, and the entire country could be covered, although further objective evaluation is necessary. Future work should also include improvements of the methodology for mapping emissions from traffic on narrow roads, modeling of temporal variations (seasonal, weekly, and diurnal), and extending the time period of this study.

Conclusions

Spatially explicit estimates of FFCO₂ emissions were prepared for the Tokyo Metropolis, with the EI being primarily compiled using a bottom-up approach. Following the 2006 IPCC guidelines, geolocation data were collected for point, line, and area sources, with the emissions mapped where possible. Detailed activity data, including the operating ratios of power plants, load factors of vessels, fossil-carbon contents of waste, and emission factors for fossil-fueled power generation, aircraft movements, navigation, and combustion processes, were utilized to improve the accuracy of emission estimates. The utilization of spatially verified national census data, regional/city specific emission factors, and emission factors for road segments, as well as the consideration of low-emission sectors, such as waterborne navigation and agricultural machinery use, were highlighted. This EI demonstrated that the Tier 3 approach could be applicable not only at a national scale but also a sub-national scale.

The total emissions from the Tokyo Metropolis in 2014 were estimated to be 44,855 Gg CO₂. The highest emission sector was road transportation (16,323 Gg CO₂), which accounted for 36.4% of the total emissions. Spatial emission patterns were compared with those of EAGrid-Japan, highlighting differences in the distributions of source types. The differences resulted mainly from the counting and mapping approaches used, and the different sector categories.

This methodology is applicable to other prefectures and can be used to cover the entire country. This EI facilitates the acquisition of information on emissions from high-emission point sources, buildings, and road segments more than other gridded datasets. It may also be used to validate other EIs and to prepare urban carbon budgets in addition to aiding policy makers in controlling GHG emissions.

Abbreviations

CO ₂
carbon dioxide
FFCO ₂
carbon dioxide emissions from fossil fuel combustion
EI
emissions inventory
GPC

Global Protocol for Community-Scale Greenhouse Gas Emission Inventories UNFCCC:UN Framework Convention on Climate Change
IPCC
Intergovernmental Panel on Climate Change
GHG
greenhouse gas
GESAPU
National geoinformation technologies, spatiotemporal approaches, and the Protocol for Reducing GHG Emission Uncertainties
EAGrid-Japan
East Asian Air Pollutant Emission Grid Database for Japan
MW
megawatt
LTO
landing and take-off
ICAO
International Civil Aviation Organization
GT
gross tonnage
MSW
municipal solid waste
CA
combustion agent
DRM
digital road map
GIS
geographic information system
TFA
total floor area
DSM
digital surface model
DEM
digital elevation model

Declarations

Ethics approval and consent to participate

Not applicable.

Consent for publication

Not applicable.

Availability of data and materials

The data supporting our conclusions are either in the paper itself or in the links listed in the references. The data product will be opened online as the publication of this article.

Competing interests

The authors declare that they have no competing interests.

Funding

This study was funded by the Ministry of the Environment, Japan, and partly supported by the Low-Carbon Research Program of the National Institute for Environmental Studies.

Authors' contributions

RC conducted the analysis of data and drafted the text. TO designed the study. MS and TO refined the text. TF provided the data of EAGrid-Japan2010. All authors contributed to improving the manuscript. All authors have read and approved the final manuscript.

Acknowledgements

We thank two referees for their review and helpful comments. We thank Shamil Maksyutov from the National Institute for Environment Studies for his valuable comments on this article.

References

1.

1. Le Quéré C, Andrew RM, Friedlingstein P, Sitch S, Pongratz J, Manning AC, et al. Global Carbon Budget 2017. *Earth Syst Sci Data*. 2018;10:405–48. <https://doi.org/10.5194/essd-10-2141-2018>.
2. UN-Habitat. The challenge. <https://unhabitat.org/topic/climate-change>. Accessed 1 Jan 2020.
3. Hoorweg D, Sugar L, Gómez CLT. Cities and greenhouse gas emissions: moving forward. *Environ Urban*. 2011;23:207–27.
4. C40. <https://www.c40.org/>. Accessed 1 Jan 2020.
5. Global Covenant of Mayors for Climate & Energy. <https://www.globalcovenantofmayors.org/>. Accessed 1 Jan 2020.
6. Greenhouse Gas Protocol. Global Protocol for Community-Scale Greenhouse Gas Emission Inventories. 2014. <http://ghgprotocol.org/greenhouse-gas-protocol-accounting-reporting-standard-cities>. Accessed 1 Jan 2020.
7. United Nations. Paris Agreement. 2015. <https://unfccc.int/process-and-meetings/the-paris-agreement/what-is-the-paris-agreement>. Accessed 1 Jan 2020.
8. United Nations. Kyoto Protocol to the United Nations Framework Convention on Climate Change. 1998. <https://unfccc.int/process-and-meetings/the-kyoto-protocol/what-is-the-kyoto-protocol/what-is-the-kyoto-protocol>. Accessed 1 Jan 2020.
9. Gurney KR, Liang J, O’Keeffe D, Patarasuk R, Hutchins M, Huang J, et al. Comparison of Global Downscaled Versus Bottom-Up Fossil Fuel CO₂ Emissions at the Urban Scale in Four US Urban Areas. *J Geophys Res Atmos*. 2019;124:2823–40. <https://doi.org/10.1029/2018JD028859>.
10. Bun R, Nahorski Z, Horabik-Pyzel J, Danylo O, See L, Charkovska N, et al. Development of a high-resolution spatial inventory of greenhouse gas emissions for Poland from stationary and mobile sources. *Mitig Adapt Strateg Glob Chang*. 2018. <https://doi.org/10.1007/s11027-018-9791-2>.
11. Gurney KR, Razlivanov I, Song Y, Zhou Y, Benes B, Abdul-Massih M. Quantification of fossil fuel CO₂ emissions on the building/street scale for a large US city. *Environ Sci Technol*. 2012. <http://doi.org/10.1021/es3011282>.
12. Feng S, Lauvaux T, Newman S, Rao P, Ahmadov R, Deng A, et al. Los Angeles megacity: a high-resolution land–atmosphere modelling system for urban CO₂ emissions. *Atmos Chem Phys*. 2016. <https://doi.org/10.5194/acp-16-9019-2016>.
13. Patarasuk P, Gurney KR, O’Keeffe D, Song Y, Huang J, Rao P, et al. Urban high-resolution fossil fuel CO₂ emissions quantification and exploration of emission drivers for potential policy applications. *Urban Ecosyst*. 2016. <https://doi.org/10.1007/s11252-016-0553-1>.
14. The Hestia Project. http://hestia.project.asu.edu/audience_researchers.shtml. Accessed 1 Jan 2020.
15. Mori Y. Development of high spatial- and temporal- resolution anthropogenic CO₂ inventory in Osaka Prefecture (Master thesis). 2016. <http://www.see.eng.osaka-u.ac.jp/seege/seege/material/2016/mori.pdf>. Accessed 1 Jan 2020.
16. IPCC. 2006 IPCC Guidelines for National Greenhouse Gas Inventories. 2007. <https://www.ipcc-nggip.iges.or.jp/public/2006gl/>. Accessed 1 Jan 2020.
17. Electrical Japan. Fossil fuel fired power generation information. 2017. <http://agora.ex.nii.ac.jp/earthquake/201103-eastjapan/energy/electrical-japan/area/13.html.ja>. Accessed 1 Jan 2020. (in Japanese).
18. Tokyo Gas Engineering Solutions. The list of plants built under the redevelopment. <http://www.tokyogas-es.co.jp/case/#anchor08>. Accessed 1 Jan 2020. (in Japanese).
19. Tokyo electric power company holdings. The list of power plants: steam and internal combustion types. <http://www.tepco.co.jp/corporateinfo/illustrated/electricity-supply/index-j.html>. Accessed 1 Jan 2020. (in Japanese).
20. Mori building. The introduction for Roppongi energy service plant. <https://www.mori.co.jp/morinow/2011/05/20110512160000002184.html>. Accessed 1 Jan 2020. (in Japanese).
21. Agency for Natural Resources and Energy. Running ratio of fossil-fueled power plants in 2014. 2015. https://www.enecho.meti.go.jp/statistics/electric_power/ep002/xls/2014/2-4-H26.xls. Accessed 1 Jan 2020. (in Japanese).
22. Agency for Natural Resources and Energy. Energy consumption and electricity generation amount by power plants. 2014. https://www.enecho.meti.go.jp/statistics/electric_power/ep002/xls/2014/4-1-H26.xls. https://www.enecho.meti.go.jp/statistics/electric_power/ep002/xls/2014/4-2-H26.xls. https://www.enecho.meti.go.jp/statistics/electric_power/ep002/xls/2014/4-3-H26.xls. Accessed 1 Jan 2020. (in Japanese).

23. Ministry of the Environment. Guidelines for Calculation Method on Greenhouse Gas Emissions. 2017. https://ghg-santeikohyo.env.go.jp/files/manual/chpt2_4-4.pdf. Accessed 1 Jan 2020. (in Japanese).
24. Ministry of Land, Infrastructure, Transport and Tourism. Annual record of airport management. 2015. <http://www.mlit.go.jp/common/001296737.xls>. Accessed 1 Jan 2020. (in Japanese).
25. Toho Air Service. Safety report for 2015: the types of helicopters. <http://www.tohoair.co.jp/english/index.html>. Accessed 1 Jan 2020. (in Japanese).
26. New Central Airservice. Safety report for 2015: the types of aircrafts. <https://www.central-air.co.jp/en/index.html>. Accessed 1 Jan 2020. (in Japanese).
27. Air Do. Safety report for 2015. <https://www.airdo.jp/en/>. Accessed 1 Jan 2020. (in Japanese).
28. All Nippon Airways. ANA group safety report for 2015. <https://www.ana.co.jp/en/jp/>. Accessed 1 Jan 2020. (in Japanese).
29. Japan Airlines. JAL safety report for 2015. <http://www.jal.com/en/>. Accessed 1 Jan 2020. (in Japanese).
30. Skymark Airlines. Safety report for 2015. <https://www.skymark.jp/en/>. Accessed 1 Jan 2020. (in Japanese).
31. Solaseed Air. Safety report for 2015. <https://www.solaseedair.jp/en/>. Accessed 1 Jan 2020. (in Japanese).
32. Starflyer. Safety report for 2015. <https://www.starflyer.jp/en/>. Accessed 1 Jan 2020. (in Japanese).
33. Flugzeuginfo.net. Aircraft types. 2017. http://www.flugzeuginfo.net/acdata_en.php. Accessed 1 Jan 2020.
34. Haneda Airport International Passenger Terminal. Domestic flight information. 2017. <http://www.tokyo-airport-bldg.co.jp/en/flight/>. Accessed 1 Jan 2020.
35. Haneda Airport International Passenger Terminal. International flight information. 2017. <http://www.haneda-airport.jp/inter/flight/showFlightScheduleSearch?langId=en>. Accessed 1 Jan 2020.
36. ICAO. Aircraft Engine Emissions Databank. 2017. <https://www.easa.europa.eu/sites/default/files/dfu/edb-emissions-databank%20v26B-NewFormat%20%28web%29.xlsx>. Accessed 1 Jan 2020.
37. FOCA. Guidance on the Determination of Helicopter Emissions. 2013. https://www.bazl.admin.ch/dam/bazl/de/dokumente/Fachleute/Regulationen_und_Grundlagen/guidance_on_the_determinationofhelicopteremissions.pdf.do. Accessed 1 Jan 2020.
38. Ministry of the Environment. The emissions from ships. 2011. <https://www.google.com/url?sa=t&rct=j&q=&esrc=s&source=web&cd=5&ved=2ahUKEWjTnbqFkpvAhXULqYKHWviAr8QFjAEegQIAxAB&url=https%3A%2F%2Fwww.env.go.jp%2Fchemi%2F>. Accessed 1 Jan 2020. (in Japanese).
39. OPRI. Investigation report on the environmental impact of PM by vessels. 2007. <http://fields.canpan.info/report/download?id=3269>. Accessed 1 Jan 2020. (in Japanese).
40. Ministry of Land, Infrastructure, Transport and Tourism. Annual report on vessels at Tokyo port. <https://www.mlit.go.jp/common/001277697.xls>. Accessed 1 Jan 2020. (in Japanese).
41. Bureau of Port and Harbor. Annual report on vessels on ports from the islands. https://www.kouwan.metro.tokyo.lg.jp/yakuwari/27kousei_7_2.xls. Accessed 1 Jan 2020. (in Japanese).
42. Clean Authority of Tokyo. Waste disposal of Tokyo 23cities: Annual report on the waste incineration plants of Tokyo in 2014. 2016. <https://www.union.tokyo23-seisou.lg.jp/gijutsu/gijutsu/kumiai/shiryo/documents/26honbun.pdf>. Accessed 1 Jan 2020. (in Japanese).
43. Ministry of the Environment. Investigation result on the municipal solid waste disposal status of Tokyo in 2014. 2017. http://www.env.go.jp/recycle/waste_tech/ippan/h26/data/seibi/city/13.xlsx. Accessed 1 Jan 2020. (in Japanese).
44. Bureau of Environment Tokyo Metropolitan Government. Investigation Report on the Status of Industrial Waste of Tokyo in 2014. 2016. https://www.kankyo.metro.tokyo.lg.jp/resource/industrial_waste/notification/investigation.files/H26houkokusyo.pdf. Accessed 1 Jan 2020. (in Japanese).
- 45.

Bureau of Environment Tokyo Metropolitan Government. Waste disposal facilities in Tokyo. 2017. https://www.kankyo.metro.tokyo.lg.jp/resource/general_waste/processing_plant/processing_plant.files/20200101_shisetsulist.pdf. Accessed 1 Jan 2020. (in Japanese).

46. Ministry of Land, Infrastructure, Transport and Tourism. Traffic Census. 2015. <http://www.mlit.go.jp/road/census/h27/data/xlsx/kasyo13.xlsx>. Accessed 1 Jan 2020. (in Japanese).

47. Japan Digital Road Map Association. Digital road map. 2017. <https://www.drm.jp/english/>. Accessed 1 Jan 2020.

48. Ministry of Land, Infrastructure, Transport and Tourism. National Land Numerical Information Download Service: Administrative zones data. 2014. http://nlftp.mlit.go.jp/ksj-e/gml/datalist/KsjTmplt-N03-v2_3.html. Accessed 1 Jun 2019.

49. Dohi M, Shinri S, Masamichi T. Renewal of the Emission Factor of Carbon Dioxide and Fuel Consumption for Motor Vehicles. Technical note of NILIM. 2012;54:40 – 5. www.pwrc.or.jp/thesis_shouroku/thesis_pdf/1204-P040-045_dohi.pdf. Accessed 1 Jan 2020. (in Japanese).

50. United States Department of Energy. eQUEST. 2009. <http://doe2.com/equest/index.html>. Accessed 1 Jan 2020.

51. Zhou Y, Gurney K. A new methodology for quantifying on-site residential and commercial fossil fuel CO₂ emissions at the building spatial scale and hourly time scale. *Carbon Manag.* 2010;1:45–56.

52. Statistics Japan. 2014 Economic Census. 2016. <http://www.stat.go.jp/english/data/e-census/index.html>. Accessed 1 Jan 2020.

53. Agency for Natural Resources and Energy. Energy-balance table of Tokyo. 2017. https://www.enecho.meti.go.jp/statistics/energy_consumption/ec002/xls/13tokyo.xls. Accessed 1 Jan 2020. (in Japanese).

54. Gately CK, Hutyra LR. Large Uncertainties in Urban-Scale Carbon Emissions. *J Geophys Res Atmos.* 2017;122:242–60.

55. Bureau of Urban Development Tokyo Metropolitan Government. Land use of Tokyo. 2014. https://www.toshiseibi.metro.tokyo.lg.jp/seisaku/tochi_c/pdf/tochi_5/tochi_all.pdf. Accessed 1 Jan 2020. (in Japanese).

56. JAXA. ALOS Global Digital Surface model (AW3D30). 2015. <https://www.eorc.jaxa.jp/ALOS/en/aw3d30/data/index.htm>. Accessed 1 Jan 2020.

57. Geospatial Information Authority of Japan, Building polygons and digital elevation model. 2017. <https://fgd.gsi.go.jp/download/menu.php>. Accessed 1 Jan 2020. (in Japanese).

58. Statistics Japan. 2015 Population Census. 2017. <http://www.stat.go.jp/english/data/kokusei/index.html>. Accessed 1 Jan 2020.

59. Statistics Japan. Investigation in 2014–2015 for counting the CO₂ emissions from households. 2016. <https://www.e-stat.go.jp/en>. Accessed 1 Jan 2020. (in Japanese).

60. Statistics of Tokyo. Investigation result on Agricultural census in Tokyo 2015. 2017. <https://www.toukei.metro.tokyo.lg.jp/nourin/2015/ng15ta1400.xls>. Accessed 1 Jan 2020. (in Japanese).

61. National Institute for Agro-Environmental Sciences. Life Cycle Assessment for Environmentally Sustainable Agriculture. NIAES Report. 2003. http://www.naro.affrc.go.jp/archive/niaes/project/lca/lca_r.pdf. Accessed 1 Jun 2019. (in Japanese).

62. Shimizu N, Yuyama Y. Analysis of the energy consumption and profitability of agricultural practice with environmental consciousness-a case study in north-eastern Chiba Prefecture. *J Rural Plan Assoc.* 2007;26:365 – 70. (abstract in English and text in Japanese) https://www.jstage.jst.go.jp/article/arp/26/Special_Issue/26_Special_Issue_365/_article/-char/en. Accessed 1 Jan 2020.

63. JAXA. Homepage of High-resolution Land Use and Land Cover Map Products. HRLULC 10 m resolution map of Japan [2006–2011] (ver.16.09). 2016. http://www.eorc.jaxa.jp/ALOS/en/lulc/lulc_index.htm. Accessed 1 Jan 2020.

64. Bureau of Environment Tokyo Metropolitan Government. Final Energy Consumption and Greenhouse Gas Emissions in Tokyo (FY 2014). 2017. <https://www.kankyo.metro.tokyo.lg.jp/en/climate/index.files/b0548c2a69e7883f1945aca50f606a92.pdf>. Accessed 1 Jan 2020.

65. Agency for Natural Resources and Energy. Actual conditions on power generation and transmission. 2017. https://www.enecho.meti.go.jp/statistics/electric_power/ep002/xls/2014/2-5-H26.xls. Accessed 1 Jan 2020. (in Japanese).

66. Tonooka Y, Kannari A, Higashino H, Murano K. NMVOCs and CO emission inventory in East Asia. *Water Air Soil Pollut.* 2001;130:199–204.

67.

Kannari A, Tonooka Y, Baba T, Murano K. Development of multiple-species 1km × 1 km resolution hourly basis emissions inventory for Japan. Atmos Environ. 2007. <https://doi.org/10.1016/j.atmosenv.2006.12.015>.

68.

Fukui T, Kokuryo K, Baba T, Kannari A. Updating EAGrid2000-Japan emissions inventory based on the recent emission trends. J Jpn Soc Atmos Environ. 2014;49:117 – 25. https://www.jstage.jst.go.jp/article/taiki/49/2/49_117/_article. Accessed 1 Jan 2020. (abstract in English and text in Japanese).

69.

Hogue S, Marland E, Andres RJ, Marland G, Woodard D. Uncertainty in gridded CO₂ emissions estimates. Earth' Future. 2016;4:225–39. <https://doi.org/10.1002/2015EF000343>.

70.

IPCC. Good Practice Guidance and Uncertainty Management in National Greenhouse Gas inventories. 2000. <https://www.ipcc-nggip.iges.or.jp/public/gp/english/>. Accessed 1 Jan 2020.

Figures

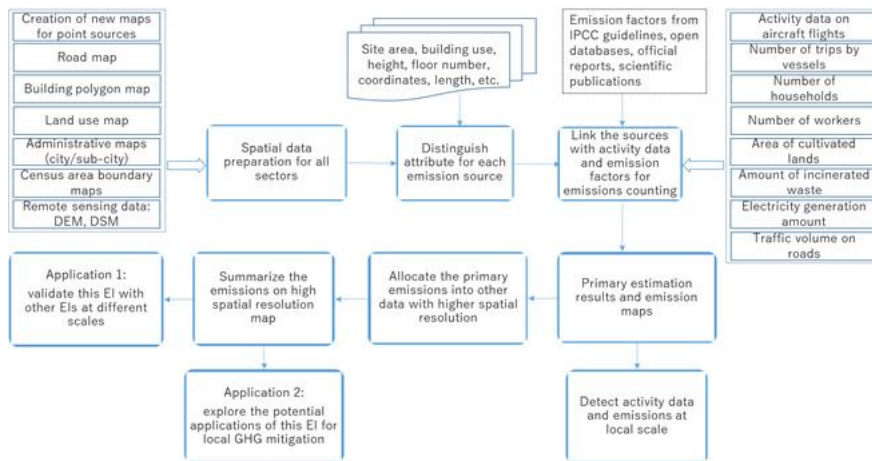


Figure 1

Conceptual framework for emission mapping

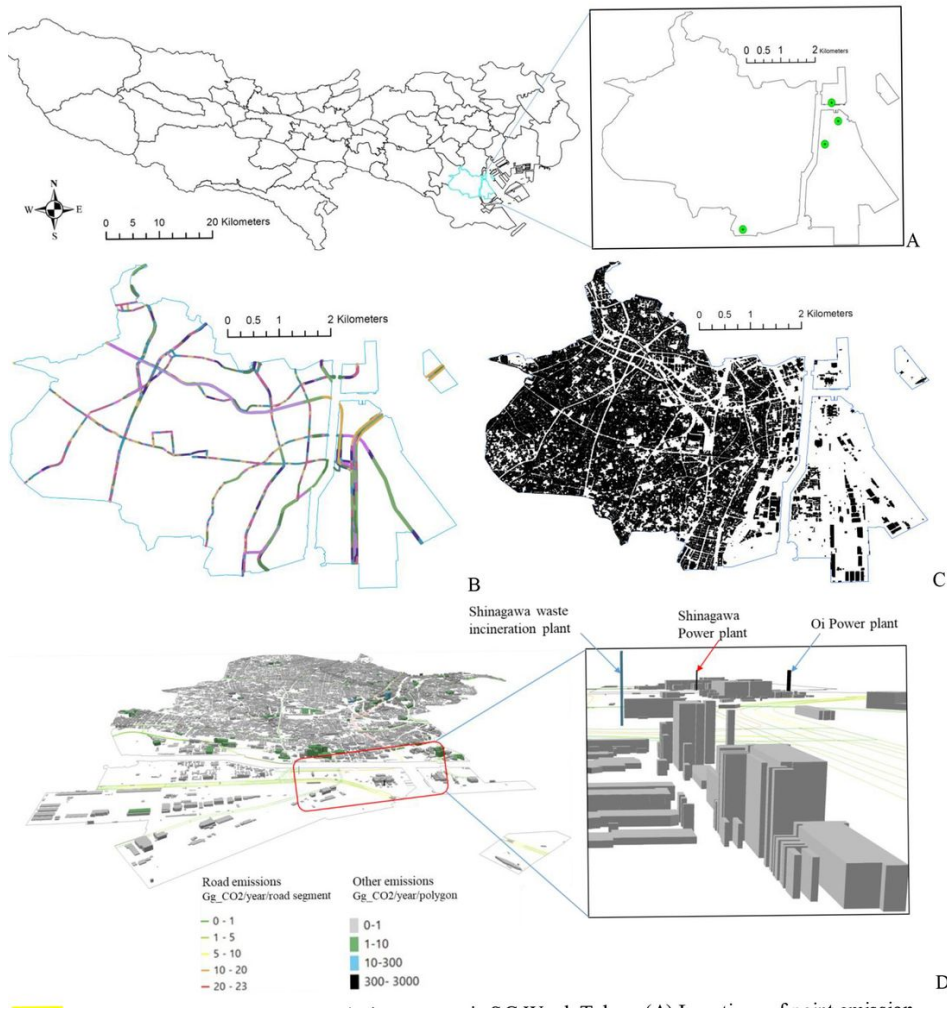


Figure 2
 Examples of vector maps for emission sources in SG Ward, Tokyo. (A) Locations of point emission sources. (B) Road segments for line sources. (C) Building polygons for area sources (blue line shows the boundary of the area). (D) 3D emission map for all sources (Gg CO₂ yr⁻¹ per road segment for road emissions; Gg CO₂ yr⁻¹ per polygon for other emissions)

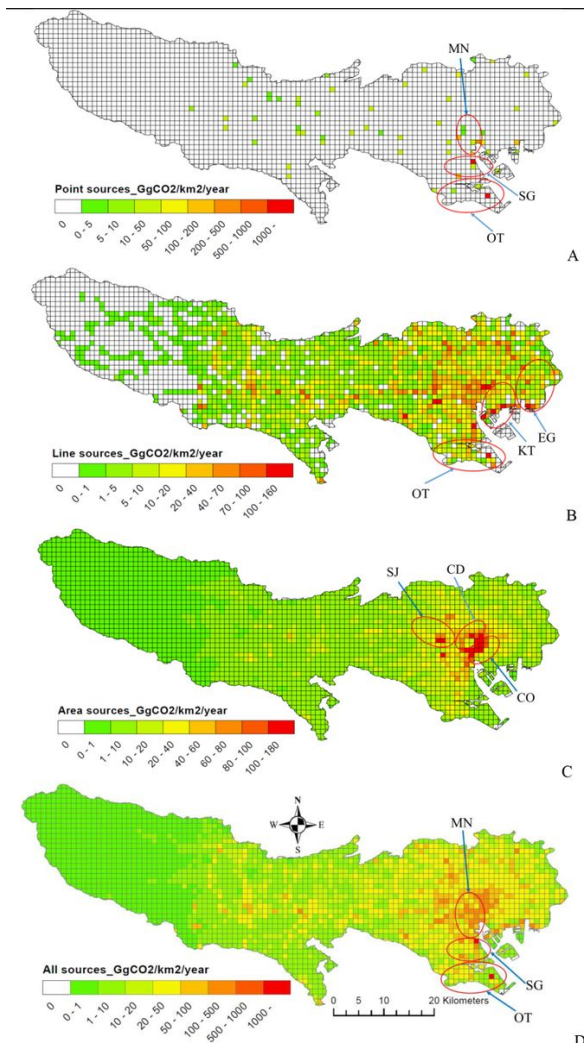


Figure 3

Emission density maps with 1 × 1 km mesh for (A) point sources, (B) line sources, (C) area sources, and (D) all sources. Unit: Gg CO₂ km⁻² yr⁻¹

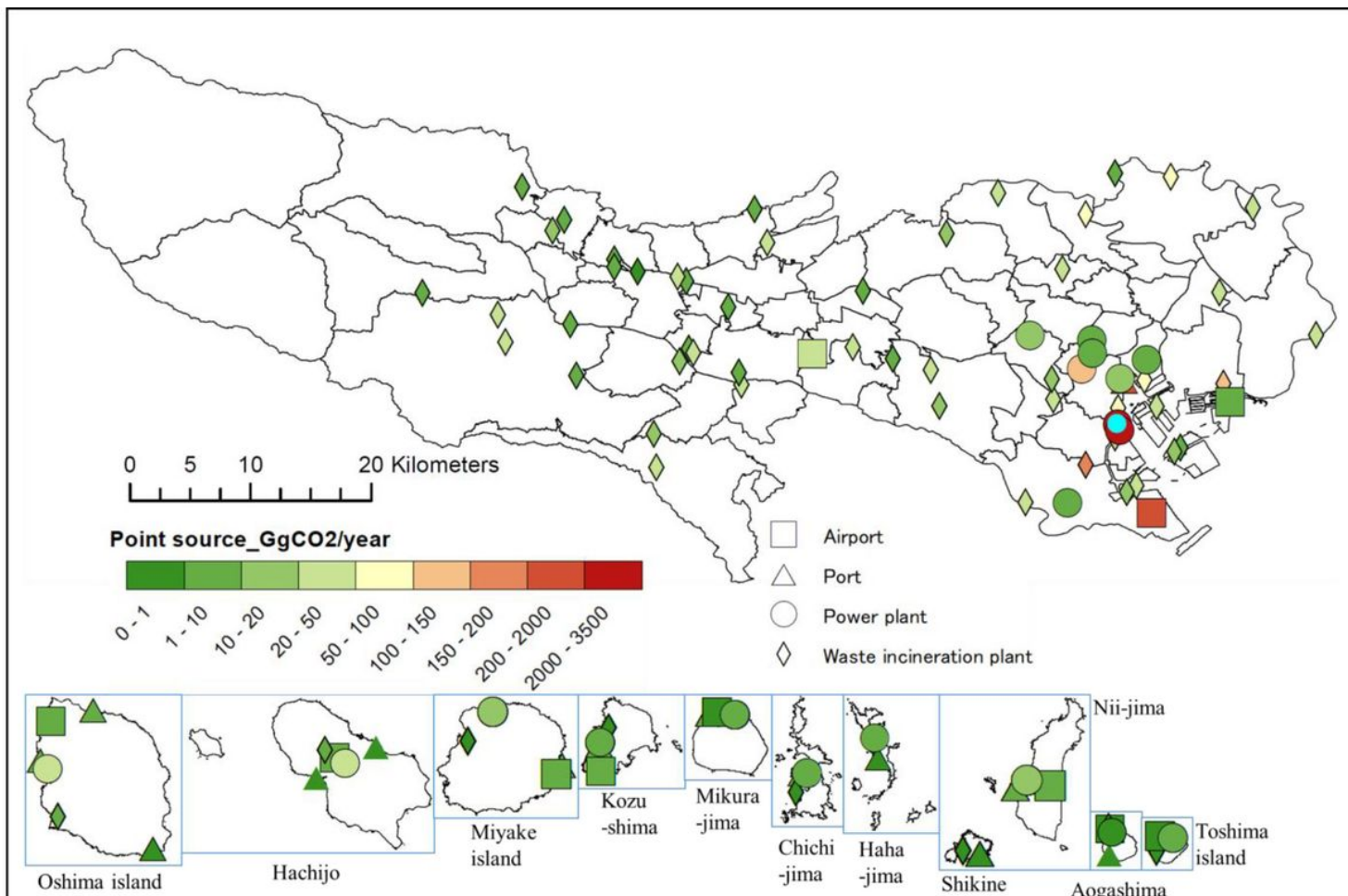


Figure 4

Map of 106 point sources in Tokyo (areas in blue frames indicate islands). The point in cyan indicates the highest emissions at Shinagawa power plant (3,219 Gg CO₂ yr⁻¹).

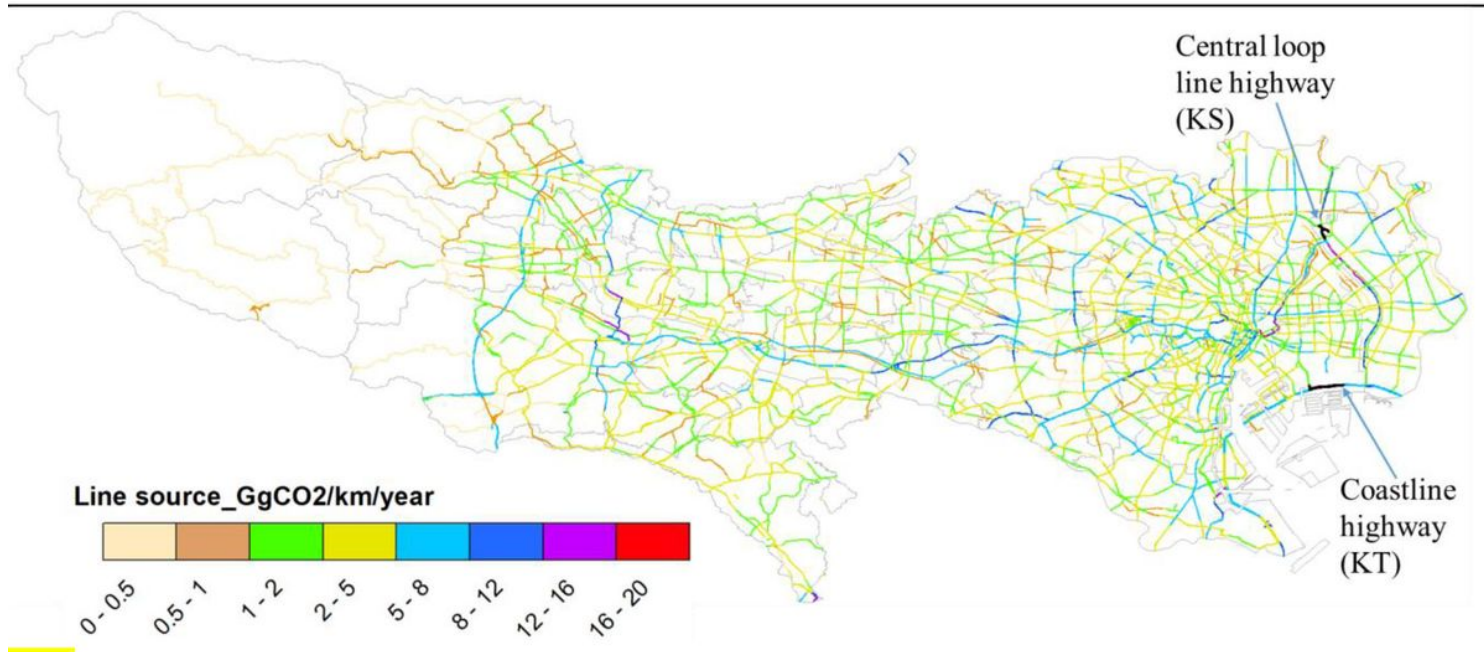


Figure 5

Map of emissions from line sources for each road segment. The 30 road segments with the highest emissions are marked in black. Unit: Gg CO₂ km⁻¹ yr⁻¹

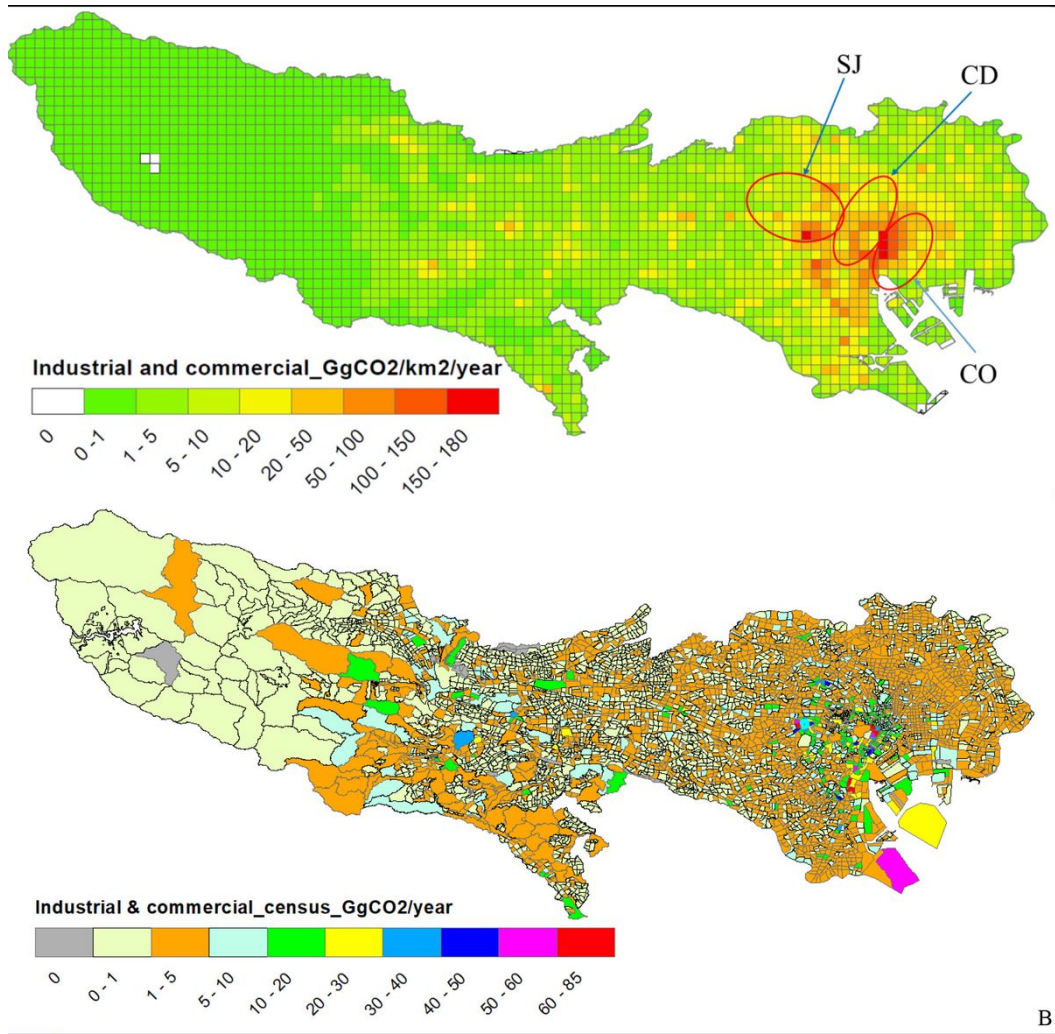


Figure 6
 Maps of emissions from the industrial and commercial sector with (A) 1×1 km mesh, unit: Gg CO₂ km⁻² yr⁻¹; (B) 5,318 economic census areas, unit: Gg CO₂ yr⁻¹. The municipality boundary for the area with the highest annual emissions (up to 82.2 Gg CO₂) is marked in cyan

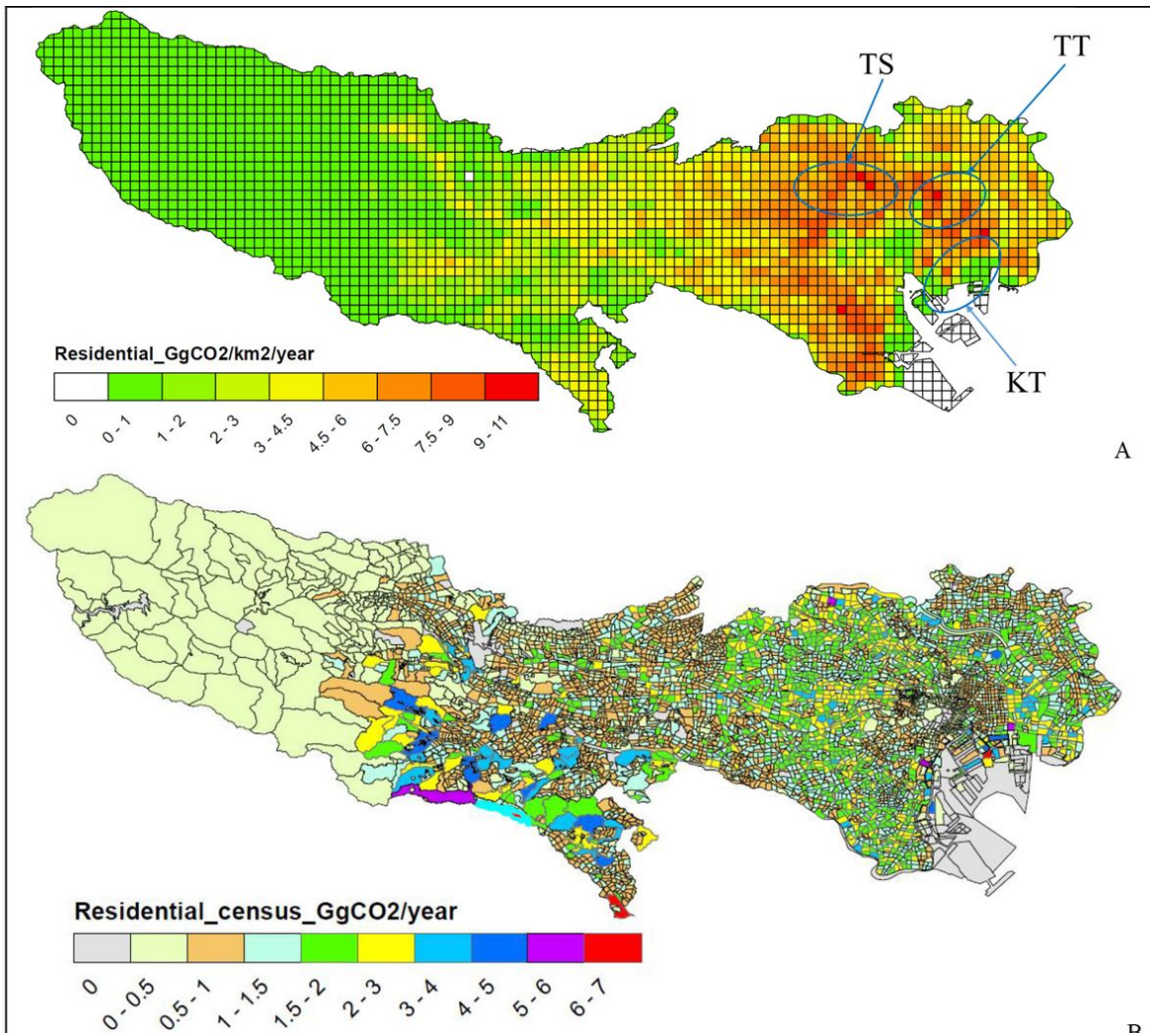


Figure 7

Maps of emissions from the residential sector with (A) 1×1 km mesh, unit: Gg CO₂ km⁻² yr⁻¹; (B) 5,578 population census areas, unit: Gg CO₂ yr⁻¹. The municipality boundary for the area with the highest annual emissions (up to 6.6 Gg CO₂) is marked in cyan

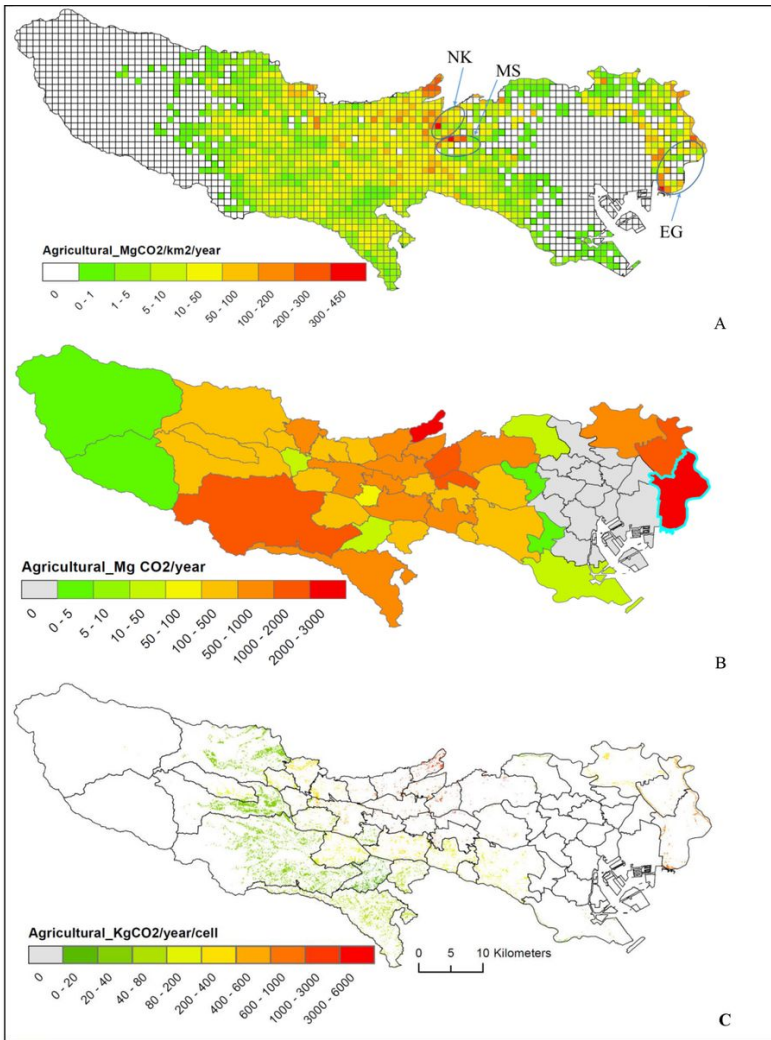


Figure 8

Maps of emissions from the agricultural machine use sector with (A) 1 × 1 km mesh, unit: Mg CO₂ km⁻² yr⁻¹. (B) 62 municipalities, unit: Mg CO₂ yr⁻¹. The area with the highest annual emissions (2,765 Mg CO₂ yr⁻¹) is marked in cyan. (C) high-spatial-resolution map on a grid with cell size of 10 × 10 m, unit: Kg CO₂ yr⁻¹ per cell

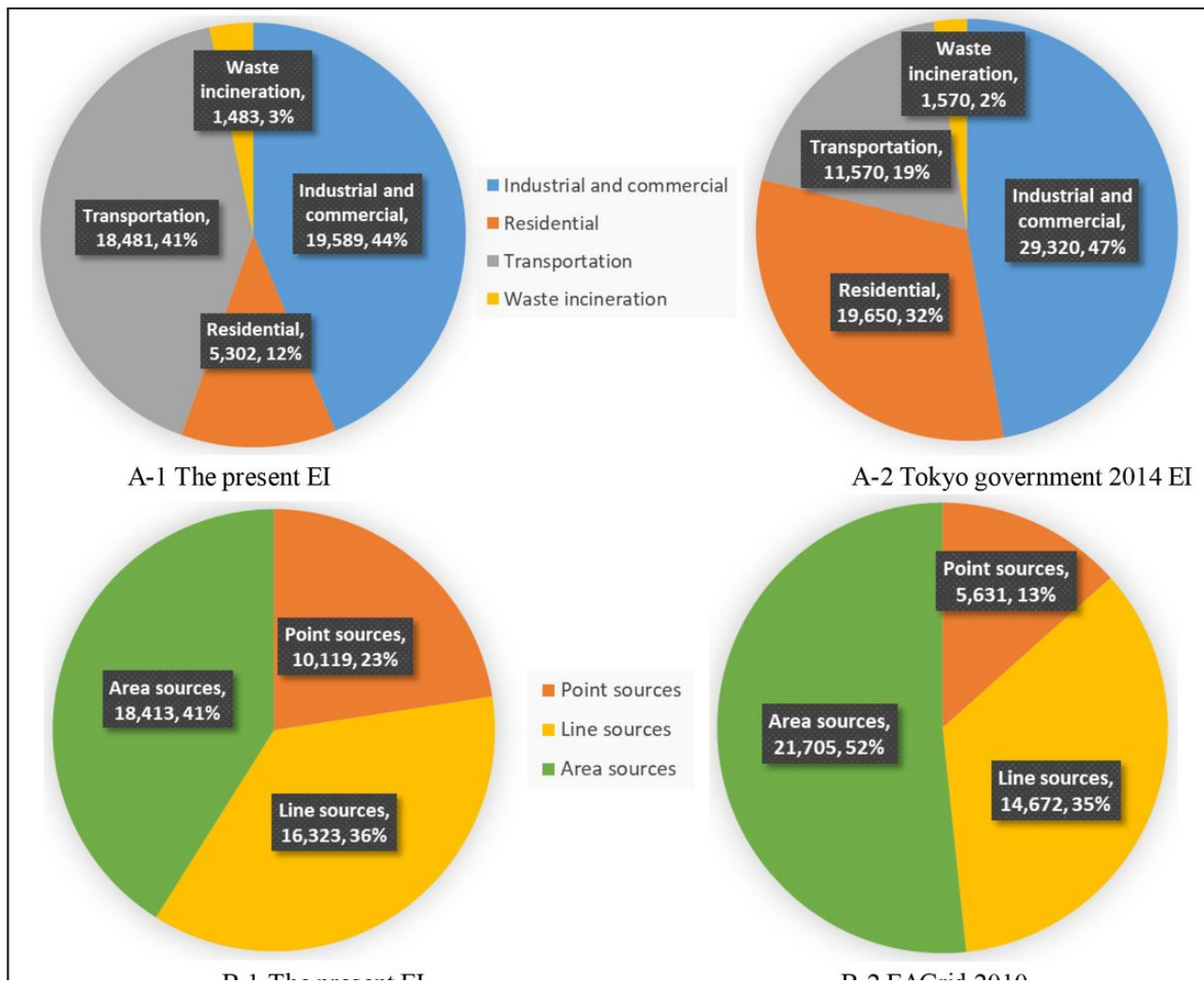


Figure 9

Comparisons on annual CO2 emissions in Tokyo between the present EI (A-1) and Tokyo government 2014 EI (A-2), and between the present EI (B-1) and EAGrid-Japan 2010 (B-2). Unit: Gg CO2 Note: In A-1, industrial and commercial category includes emissions from the industrial and commercial sector and the electricity generation sector. The transportation category includes emissions from the road transportation, civil aviation, and waterborne navigation sectors. In A-2, the transportation category includes emissions from the railways, road transportation, civil aviation, and waterborne navigation sectors. In B-2, point sources include power plants, waste incineration plants, vessels, and aircrafts. Line sources refer to road transportation. Area sources include residential and commercial combustion equipment, factory and building boilers, off-road transportation, open burning, and facilities without identified locations.

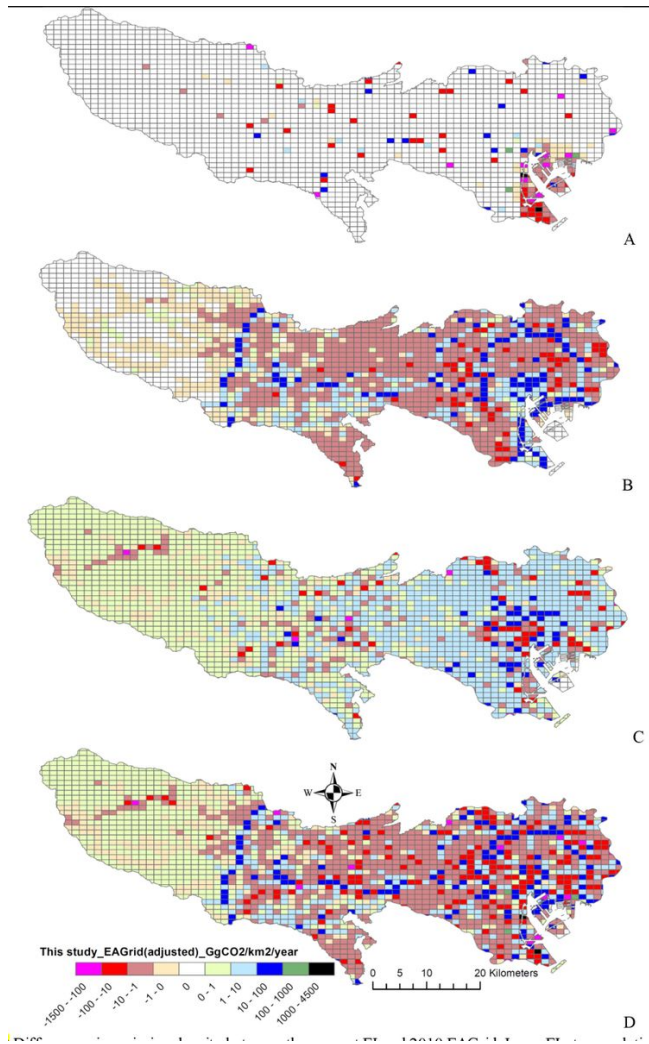


Figure 10

Differences in emission density between the present EI and 2010 EAGrid-Japan EI at a resolution of 1 × 1 km for: (A) point sources, (B) line sources, (C) area sources, and (D) all sources. Unit: Gg CO₂ km⁻² yr⁻¹. (Difference = emission density from the present EI – 2010 EAGrid-Japan EI, after adjustment of EAGrid emissions, as described in the text.)

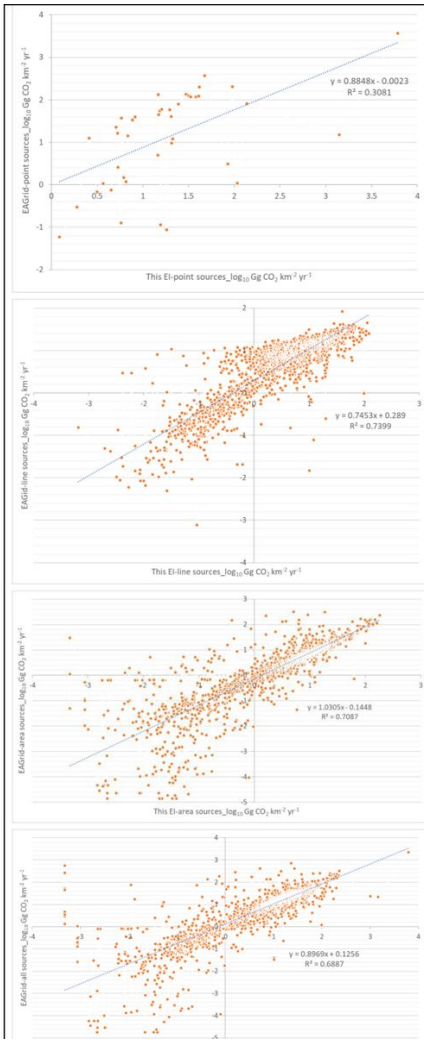


Figure 11

Scatter plots of gridded emissions by source types between the present EI and EAGrid for: (A) point sources, (B) line sources, (C) area sources, and (D) all sources. Unit: $\log_{10} \text{ Gg CO}_2 \text{ km}^{-2} \text{ yr}^{-1}$

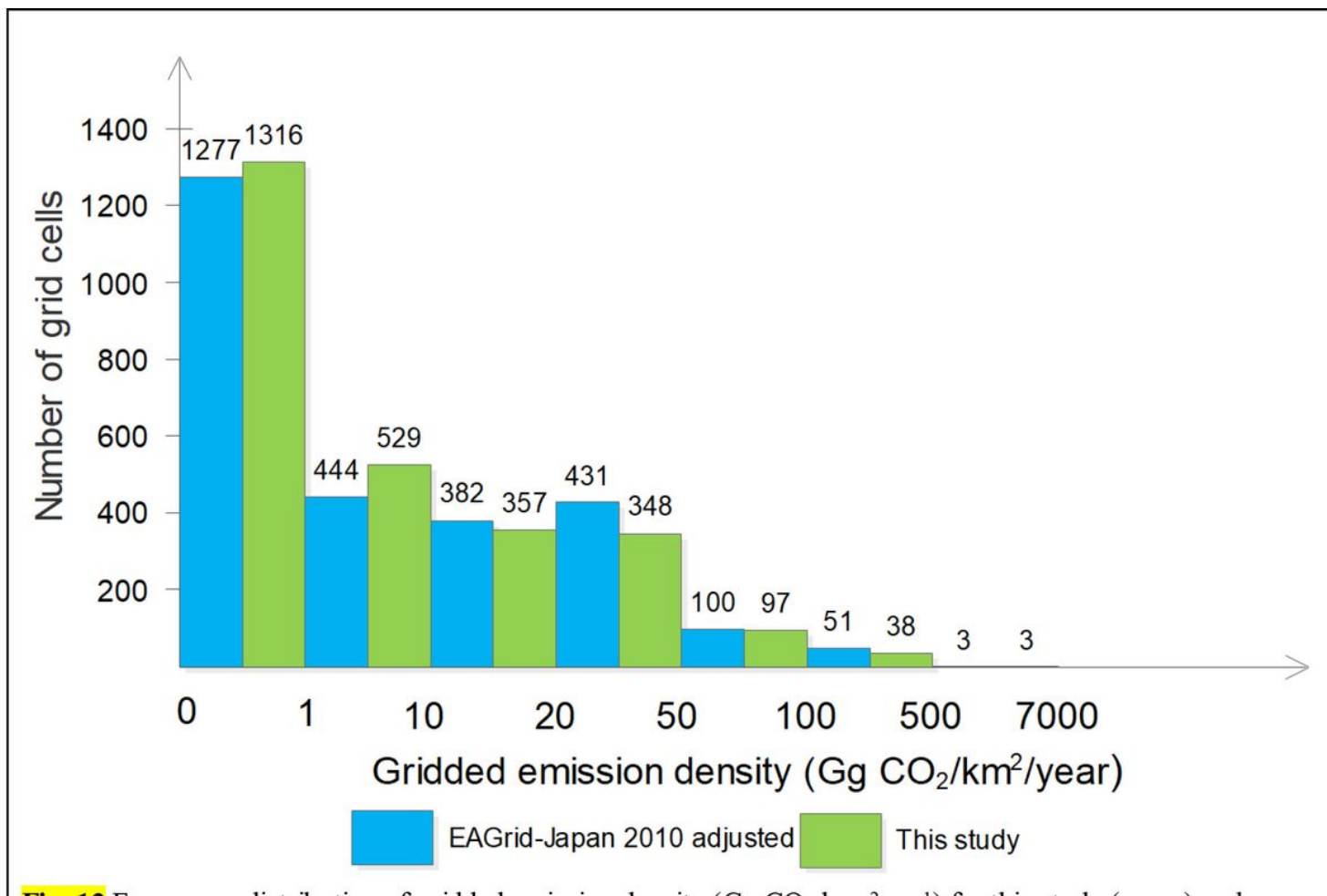


Figure 12

Frequency distribution of gridded emission density (Gg CO₂ km⁻² yr⁻¹) for this study (green) and EAGrid-Japan 2010 adjusted (blue). n = 2,684

Supplementary Files

This is a list of supplementary files associated with this preprint. Click to download.

- [SuppFinal.docx](#)